

Design and Analysis of a Fast Steering Mirror for Precision Laser Beams Steering

¹Qingkun ZHOU, ²Pinhas BEN-TZVI and ¹Dapeng FAN

¹ College of Mechatronics Engineering and Automation, National University of Defense Technology,
Changsha Hunan 410073, P. R. China

² Department of Mechanical and Aerospace Engineering, School of Engineering and Applied Science,
The George Washington University, 801 22nd St., NW, Washington, DC 20052, USA

Tel.: (202) 994-6149

E-mail: zqkhome@gmail.com, bentzvi@gwu.edu

Received: 29 January 2009 /Accepted: 22 February 2009 /Published: 23 March 2009

Abstract: Precision laser beam steering is critical in numerous applications. Also, precise pointing of laser beams is essential in challenging environments. The optical signal may be deflected, drift and wander due to environmental influences. The core problem of steering performances is to deal with the jitter disturbance. Based on the analysis of the beam angle steering system, some important factors to design the structure of a Fast Steering Mirror (FSM) and the layout of laser optics steering system are presented. Flexure hinges with compliant mechanisms are used to build the FSM structure. A 4-quadrant detector is used as the sensor for the incoming light. A design of the developed control loop and concepts of the FSM model are discussed. A comparison between the measured gain response and the simulation model of the FSM reveals similarity between the theoretical simulation model and the real system, and offers a way to improve the model to better resemble the real system. A laser beam jitter control test bed is also introduced to improve jitter control techniques. *Copyright © 2009 IFSA.*

Keywords: Precision laser beam steering, fast steering mirror, flexure hinges, optical focusing control, jitter compensation.

1. Introduction

Laser beam steering is an important technology, which plays a central role in contemporary technological applications, such as high-energy laser systems (HEL), free-space optical communications, semiconductor manufacturing and inspection, laser welding and cutting of materials

processing, optical data storages and information display, scanning optical lithography and various medical applications for biomedical systems [1], [2]. The precise optical communication is becoming a better alternative over radio communication. It provides ways to increase the data rate that is limited by the capabilities of traditional radio links. It also requires smaller divergence beams and thus smaller size of the communication terminals, and also requires less power than traditional radio wave transceivers. For instance, successful laser communication tests have been performed between two satellites in space and between a satellite and a ground based fixed partner [3]. The higher speed transmission optical communication is accomplished by laser point to point links. In order to initiate it, the two partners need to know each other's position and according to it to align their transceivers [4-6]. Precise pointing of laser beams is often required in challenging environments where disturbances like base-motion vibrations, fast relative motion and disturbances within the medium of propagation (e.g., atmospheric turbulence) occur. Such environmental conditions may induce laser beam jitter that poses critical performance limitations, and even small disturbances often produce significant jitter due to amplification by optical path lengths [7-10]. The optical signal break-up and wander is caused by environmental influences. The turbulent atmospheric effects cause the various parts of an image to arrive at different times, which results in wave front errors [11]. Vibrations or thermally-induced motion can blur precise images, reduce critical intensities, and misalign interfaces between laser and target, leading to severely compromised system performance. In order to maintain the communication, the two optical communication terminals have to track and perform precise continuous pointing to each other so that no data is lost. These increase the requirements towards the precise pointing of laser beams high-bandwidth rejection of disturbances produced by turbulence. The wavefront errors are compensated with a technique called adaptive optics. FSM is used to deal with the line-of-sight control problem in laser beam steering applications. This technique was originally developed for military and aerospace applications, such as the airborne laser (ABL) and advanced tactical laser (ATL) [6], [7], [12]. FSM presents more challenges in terms of the need for extremely precise pointing between the two partners involved in the link. They have recently been used as active mirror elements in high-performance beam-stabilization, laser beam steering and alignment modules. These modules provide a feasible approach to system performance improvement. The FSM model and closed loop control are derived and the Bode diagrams are compared in order to make clear the design considerations and the difference between the model assumptions and the experimental results. The goal is to build a beam steering system using a FSM based on compliant mechanisms and electromagnetic actuators to maintain precise laser beams steering control.

2. FSM Design and Considerations

A study over of the possible technologies for precision laser beam steering leads to the following ones: FSM, acoustic-optic deflectors [13], spatial light modulators (SLM), and deformable mirrors (DM), [14]. Angular beam steering, presented in Fig. 1 can fulfill the important steering requirement such that the laser beam will follow the ideal position. Precise rotations along one or two axes are performed by using the devices at the optical path. There are two kinds of mirrors to perform the steering: one dimensional mirror (to perform rotation about one axis only - 1D) and two dimensional mirrors (to perform rotation about two axes - 2D).

The FSM is represented as a mirror that is mounted over the actuators, as shown in Fig. 2. The actuators are capable of producing fast and precise movements. For the purpose of performing tilting around the axis, the mirrors are linearly arranged in sets of two per axis. The origin of the coordinate system is located in the center of the mirror. The linear actuators produce an angular torque that creates a small rotation about the X axis, as depicted in Fig. 2.

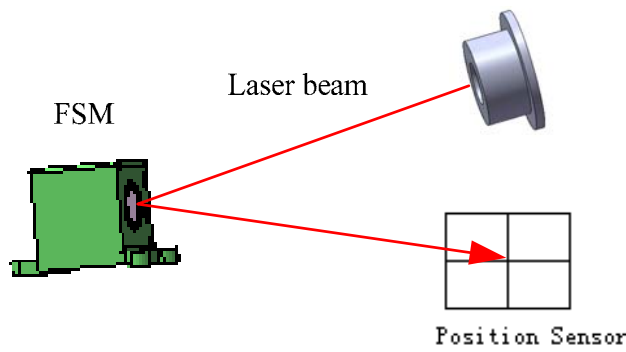


Fig. 1. Angular beam steering.

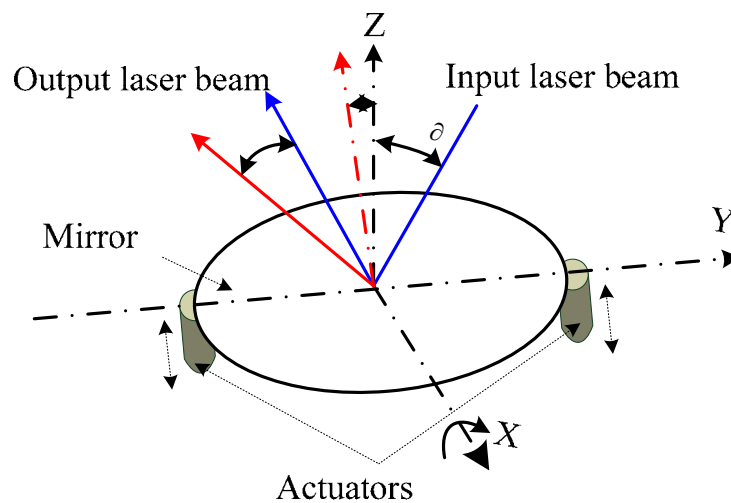


Fig. 2. Fast steering mirror principle.

The rotation positions the mirror at different angle α to reflect the input laser beam [15], [16]. The change of the optical angle of the output beam, as shown in Fig. 3, is twice the change in the mechanical angle around one axis of the XY plane.

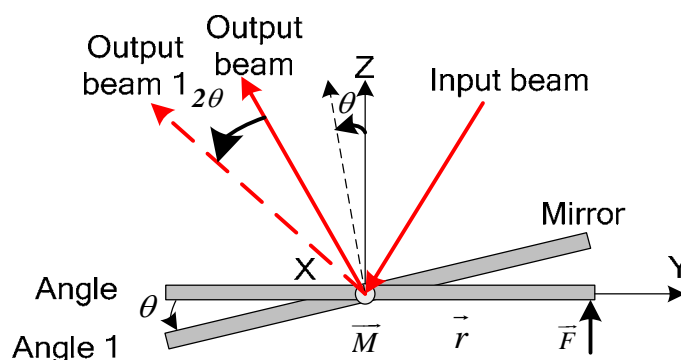


Fig. 3. Range relationship of steering angle.

Compliant mechanisms (CMs) are mechanical devices that provide smooth and controlled motion guidance due to the deformation of some or all of the mechanism's components. CMs do not require sliding, rolling or other types of contact bearings often found in rigid mechanisms. These characteristics

enable CMs to achieve reliable, high-performance motion control at low cost. Flexure hinges (Fig. 4) are the main constituents of compliant mechanisms. The flexure hinges, alternatively called flexural pivots, consist of a flexible, slender region between two rigid parts that must undergo limited relative rotation in a mechanism (which will be called compliant) due to the presence of at least one flexure hinge. Under the combined action of external loading and actuation, the flexure hinge bends and thus produces the relative rotation between the adjacent members. Being monolithic with the rest of the mechanism for the vast majority applications, flexure hinges hold several advantages over classical rotational joints [17], [18]. These include: no friction losses, no need for lubrication, no hysteresis, compactness, capacity to be utilized in small-scale applications, ease of fabrication, virtually no assembly, and no maintenance requirements.

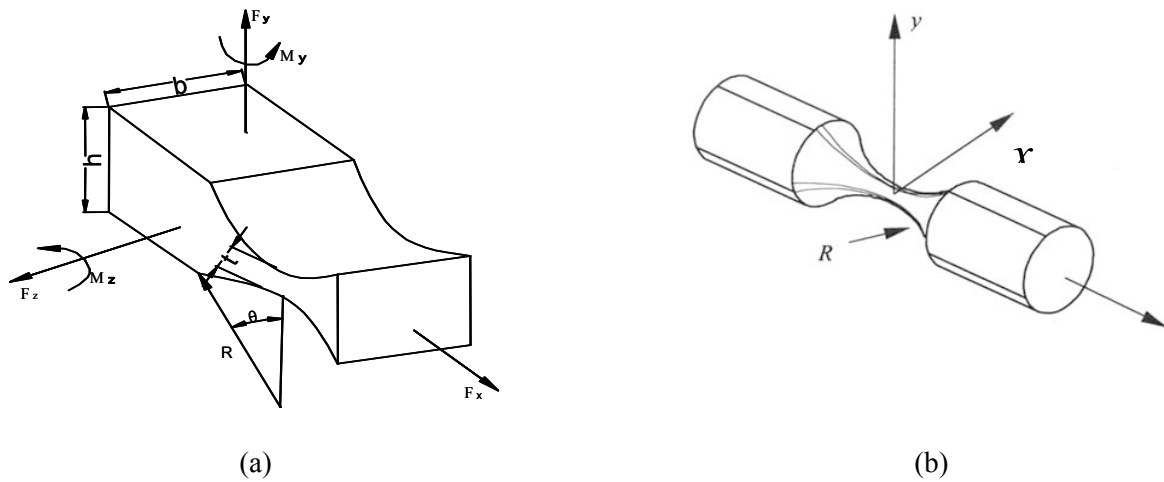


Fig. 4. Flexure hinges: (a) single axis flexure hinge with rectangular cross-section, (b) multi-axis flexure hinge (revolute).

The compliant structure of the FSM with flexure hinges is shown in Fig. 5. Several technologies are used to actuate the mirror tilting: motorized actuators, galvo motors, piezo actuators, and voice coil actuators.

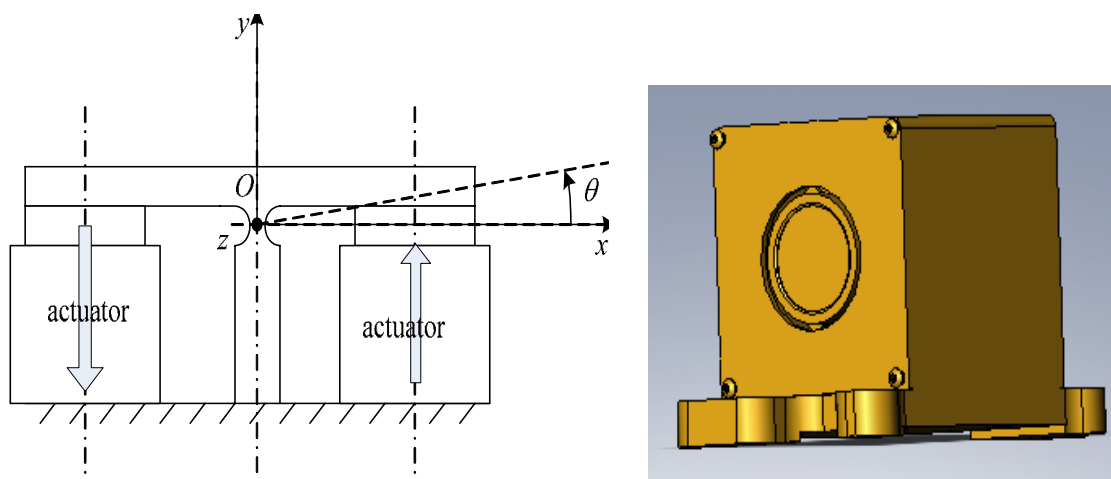


Fig. 5. Compliant structure of FSM with flexure hinges.

A beam steering system is made of the following components [19]: (i) Fast steering mirror - in our case a flexure suspended single or two axis voice coil mirror; (ii) Optical Beam-splitter – a half silvered flat

mirror that reflects some percentage of a laser beam while also transmitting another portion of it; (iii) Position Sensing Detector (PSD) – either a lateral effect cell that outputs a voltage proportional to beam placement, or a quad cell that splits up the detector into 4 quadrants; and (iv) Imaging or focusing lenses – used either to transform angular error into displacement or to re-image an angular source. The actuator in this case is the FSM mirror, while for the sensor there are several types that might be appropriate: CCD camera, PSD, photodiodes, etc. Here, a 4-quadrant detector (4QD) (Fig. 6) has been used since it is convenient for centering applications [20]. It consists of 4 photodiodes forming a circle. Their output is used to evaluate the position of the spot on the detector.

The four sectors of the 4QD are represented by letters A, B, C, and D as shown in Fig. 6. Equation (1) is used to describe the x and y displacements of the beam, where A, B, C, and D are the currents generated by each of the four sectors. There are two significant restrictions on the beam motion used with quadrant detectors. First, to provide x - y data, the beam must always overlap a portion of all four sectors. Second, there is meaningful absolute position information only for small displacements of the beam.

$$x = \frac{(B+C)-(A+D)}{A+B+C+D} \quad y = \frac{(A+B)-(C+D)}{A+B+C+D} \quad (1)$$

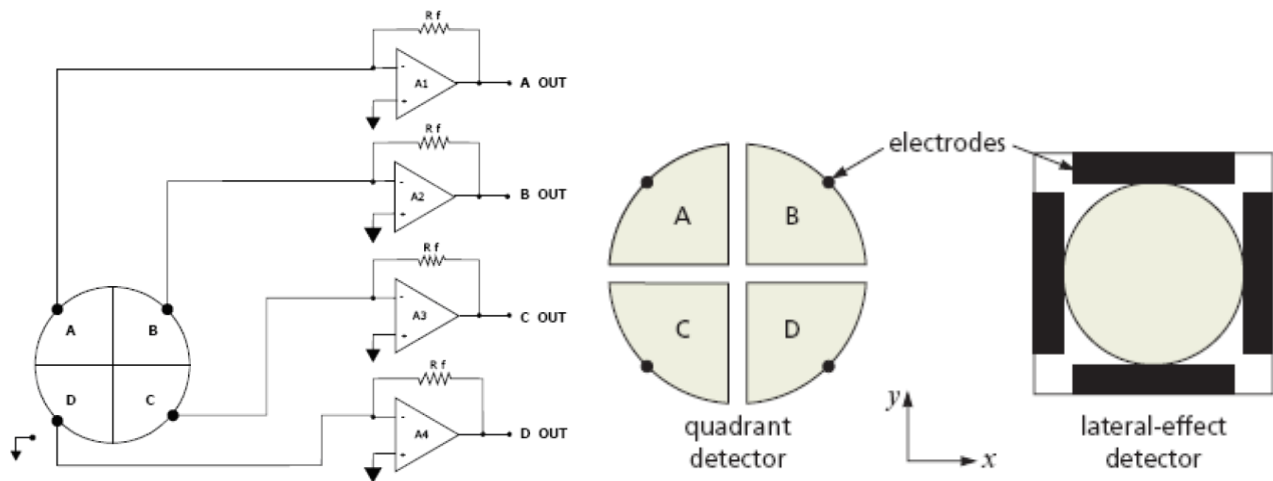


Fig. 6. Principle of Quad cell.

3. System Modeling and Simulation

In the precise laser beam steering system it is necessary to align a laser beam to a target and maintain the alignment with extreme precision over long periods of time. In order to accomplish this requirement, the control loop shown in Fig. 7 is proposed [19]. An active feedback loop maintains alignment by nulling the beam to the center of the target. Because the center of a quadrant detector does not change with time or temperature, the quadrant detector senses even small drifts of the beam away from the center. With the high resolution and accuracy of the 4QD, nulling is controlled by a computer that processes the signals from the detector and adjusts a pointing mirror to re-center the beam.

The simplest implementation of a beam stabilizer consists of a FSM, a beam-splitter, and a position sensing detector. The laser is reflected off the FSM and then passed through a beam-splitter. The majority of the energy is reflected and a small percentage of it is passed through the beam-splitter. The energy that passes through the beam-splitter is directed onto a quad cell.

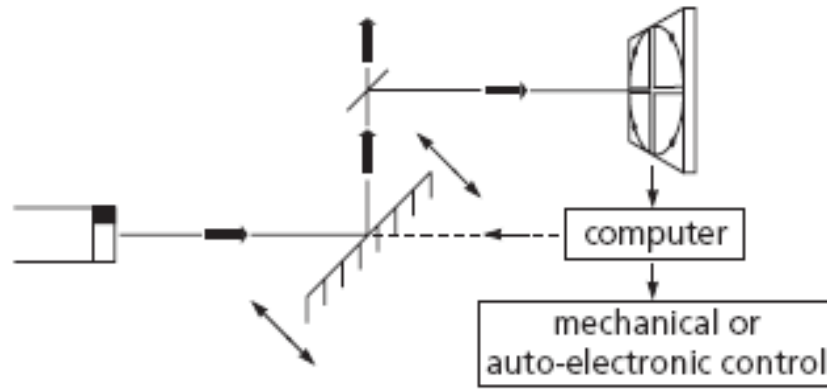


Fig. 7. Diagram optical beam alignment.

As the laser beam drifts, the spot on the quad cell moves off center. Feedback from the quad cell causes the FSM to correct this motion and move the beam back to the center of the quad cell. The result of this correction is that the beam is held fixed at a point in space (the center of the quad cell). This may be an acceptable condition, but the beam angle is not controlled. In fact, depending on the distance from the FSM of the angular error source compared to the distance from the quad to the FSM, the angular error may even be magnified. To eliminate this angular error, a focusing lens can be added in front of the quad cell, as shown in Fig. 8. This lens is located one focal length away from the quad cell. This lens has the effect of eliminating beam translation errors from the quad cell output [21]. Only beam angle change causes the spot to move on the quad cell. The angular range and resolution is set by the choice of the quad cell and the focusing lens.

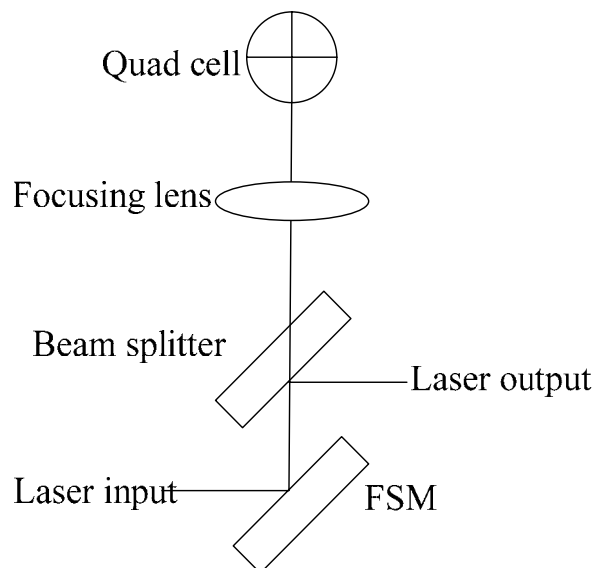


Fig. 8. Single FSM steering with Focus Lens.

The two FSM axes are controlled independently. Since the control loop of each of the FSM axes looks alike, only one axis loop is shown in Fig. 9.

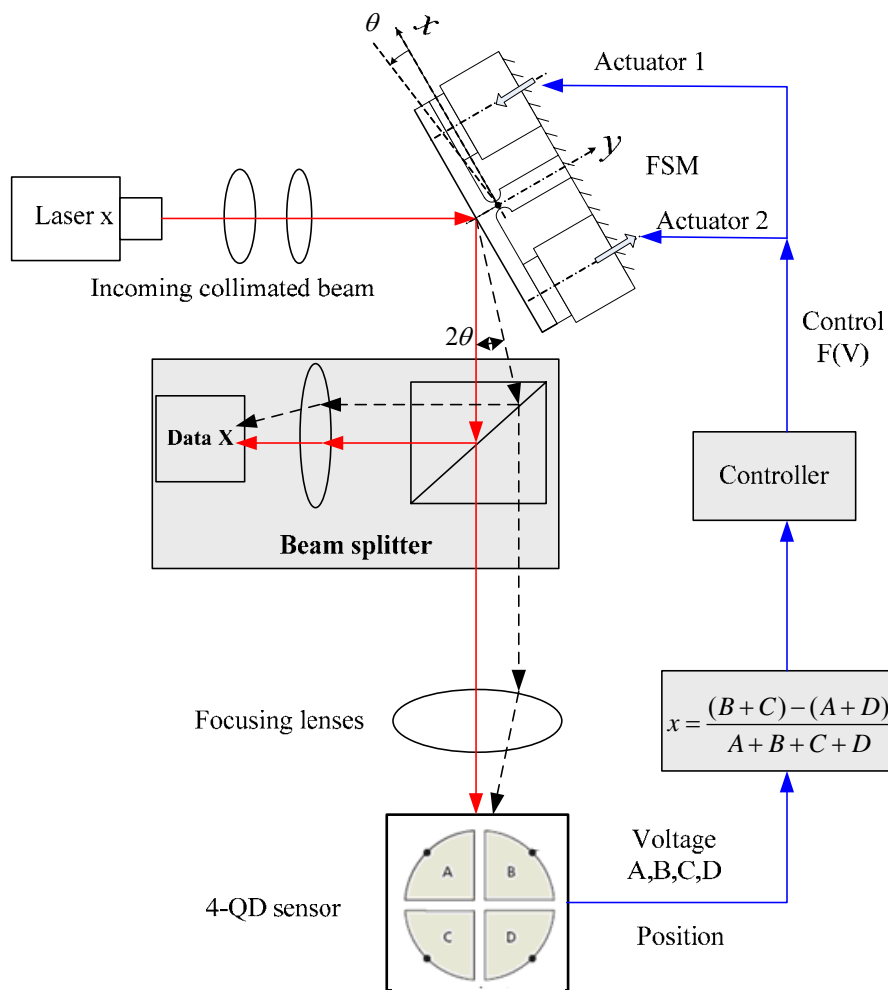


Fig. 9. Single control loop block diagram for 1-axis control.

The system input is the incoming collimated beam, while the output is the light focused on a photodiode. The collimation of the beam is generally done before it enters the pointing system. The beam is reflected by the actuator and subsequently split by the beam splitter in two directions: one beam is focused on a photodiode and the other is focused on the 4QD. The output of the 4QD is the feedback signal for the control loop [22]. When testing the control part only, the beam splitter and the fiber coupler are excluded from the system for the sake of simplicity since they do not influence the performance of the pointing. The control loop relies on the information coming from the quadrant detector. Each photodiode converts the incoming light into current, which is then converted into voltage. The 4 outputs are then used to calculate the central point of the beam onto the detector, which in its turn is fed into the controller. According to the position of the centre, the controller generates operating signals for the fast steering mirror in order to rotate it in the required orientation.

In order to correct both angle and displacement errors, two FSMs are needed as illustrated in Fig. 10(a). The core of the system is composed of the two FSMs and two position detectors, which give feedback to the FSM's controller to keep the beam locked at the center. FSM1 corrects for angle due to the feedback it receives from Quad Cell 1 and FSM2 corrects for position due to the feedback it receives for Quad Cell 2. An additional construction, shown in Fig. 10(b), uses two FSM steering systems, two beam-splitters, and two quad cells. The distance from FSM 1 to FSM 2 is equal to the distance from FSM 1 to Quad Cell 1. This ensures that the beam is stationary on the surface of FSM 2. An additional beam-splitter samples the beam and sends it to Quad Cell 2. FSM 2 removes the angular beam error.

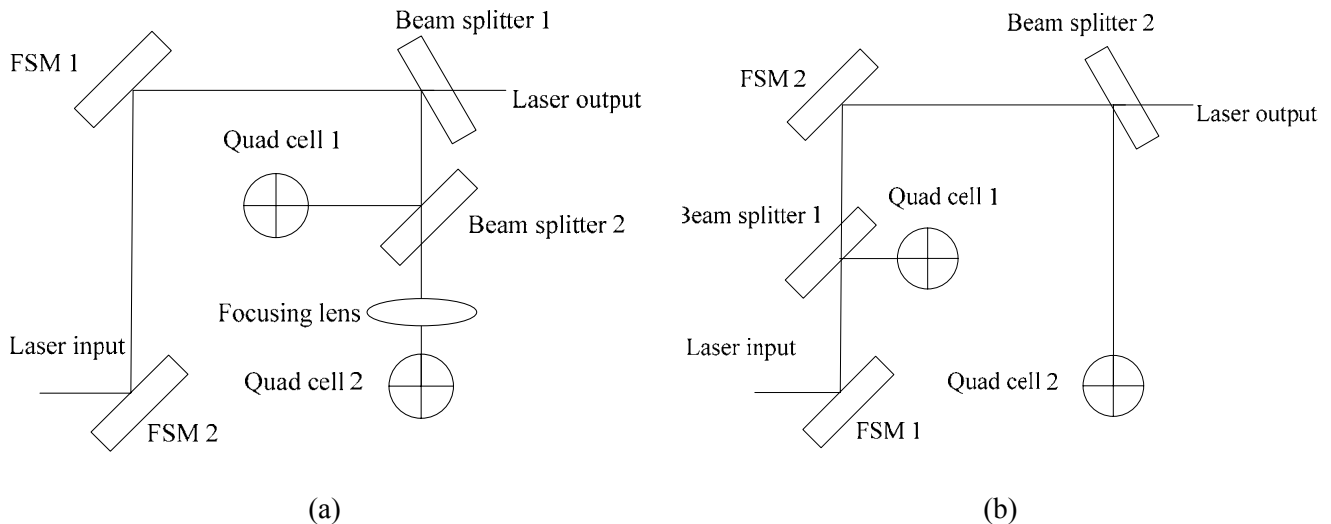


Fig. 10. Two FSMs laser beam steering.

In order to address the jitter problems as mentioned in the introduction part, two FSMs can be used for the system setup as shown in Fig. 11. The main optical components in the experiment are the laser source, two fast steering mirrors, controller and position sensing device [23]. The laser beam leaves the fixed source and reflects first off the mirror FSM 1, which adds disturbance to the beam direction, the beam then reflects off the mirror FSM 2, which serves as the control actuator, and finally goes to the sensor. A lens between FSM 1 and FSM 2 and another lens between FSM 2 and the sensor focus the beam to maintain small spots on FSM 2 and the sensor. There are two sources of jitter in the experiment: the shaker on which the control actuator is mounted and the disturbance actuator FSM 1. The motion of the shaker is vertical, and FSM 1 adds jitter on both mirror axes. A laser source is used as a replacement of a laser communication transmitter. The mirror used to produce distortions on the beam direction was aligned at 45° angle of incidence to the incoming beam, as depicted in Fig. 11. The deflected light then reaches the controlled mirror, which is also at 45° and directs the beam through the focusing system into the four quadrant detector active area. The photodiodes convert the incoming light into currents which after the amplifier board are sent as voltage signals to the filter board. Then the four information signals are digitized and used in the controller calculations to produce control signals for the actuator. They are converted to analogue signals and sent to the mirror driver, which in its term controls the rotation of the mirror.

The iterative algorithm shown in Fig. 12 is proposed for eliminating the high frequency noise by using a low-pass filter placed before the analogue to digital converter. Two signal paths can be identified: optical signal path and electronic signal path; with the two paths meeting at each end of the control loop, at the sensor and at the actuator.

With the condition that the internal assembly of the designed FSM is not coupled, the FSM can be modeled as a 2nd order linear differential equation that describes the movement of the mirror around the flexure hinge axis. The mirror assembly basic elements include the mirror itself and a flexure mount to which the mirror is attached. The FSM is actuated by 2 voice coil actuators, which are linear and work in pairs to produce rotation around the flexure hinge axis. According to these conditions, a simpler representation of the systems that involves a spring and a damper can be used. A sketch of such a spring–mass–dashpot system is presented in Fig. 13. The spring in the real device accounts for the oscillations and is related to the flexure (hence accounts for the elasticity of the flexure). The damper accounts for the smooth movement and is related to the air viscosity [24].

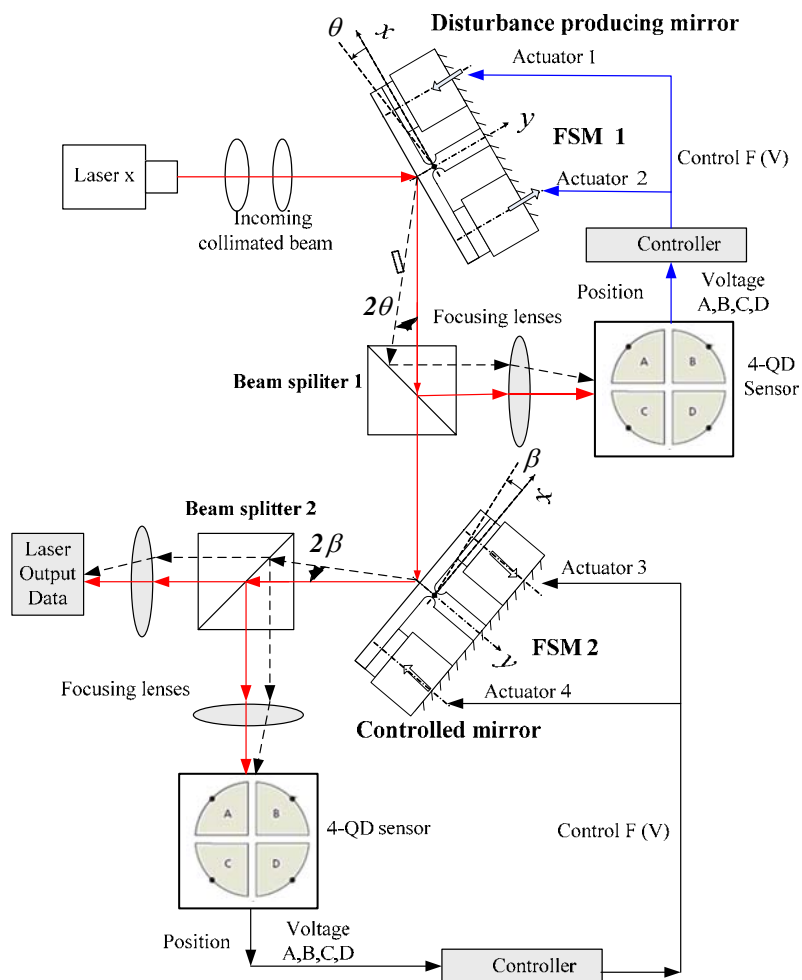


Fig. 11. Two FSMs Laser Beam Steering (FSM1 for distortion and FSM2 for active control).

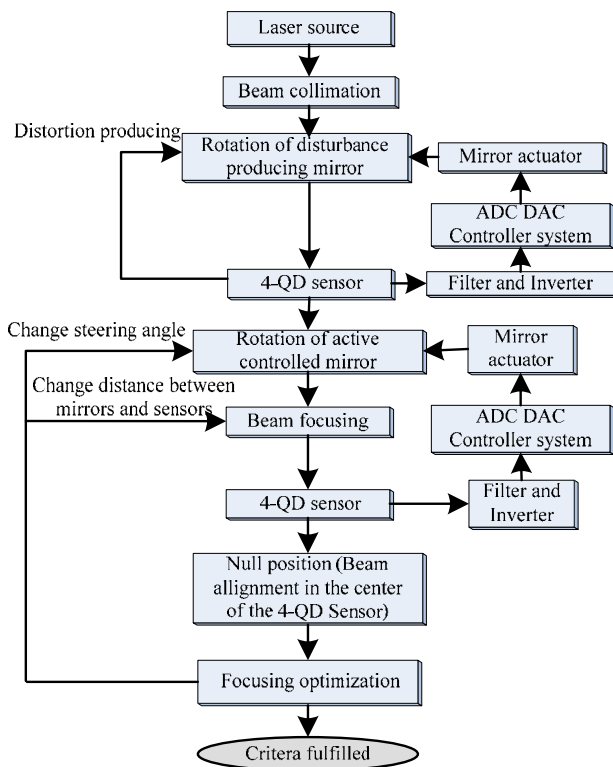


Fig. 12. Optical setup block diagram.

As shown in the Fig 13, the dimension d of the mirror itself is designed and depends on where the actuator pushes the mirror. In order to derive the Laplace transform of the theoretical model of the FSM, we assume that the actuators act on the mirror at the mirror's end.

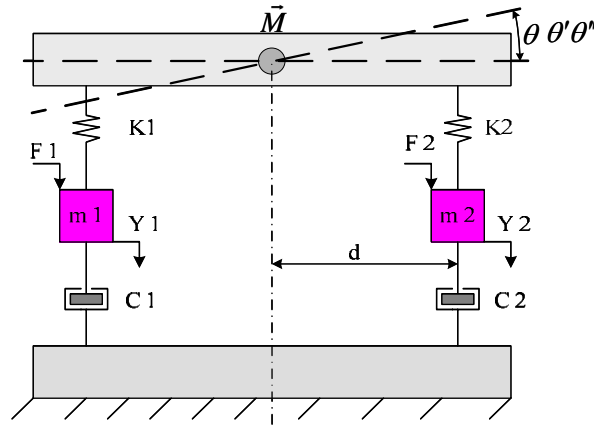


Fig. 13. A sketch of the spring-mass-dashpot system.

The differential equation describing the system is given by:

$$M = [J + (m_1 + m_2)d^2]\theta'' + (C_1 + C_2)d^2\theta' + (K_1 + K_2)d^2\theta \quad (2)$$

where m is the mass of the mirror itself and a flexure mount; k is the spring constant; and c is the viscous damping coefficient. In order to describe the behavior of the system, the transfer function $G(s)$ is derived to relate the output to the input:

$$G(s) = \frac{\theta(s)}{M(s)} = \frac{1}{s^2 + \frac{(C_1 + C_2)d^2}{J + (m_1 + m_2)d^2}s + \frac{(K_1 + K_2)d^2}{J + (m_1 + m_2)d^2}} \quad (3)$$

The torque M is used as input parameter but the force F may be modeled as the response of the actuator and be produced by the pair of voice coil actuators. It receives voltage commands and converts them to four current commands (which in their turn are relative to the force F) in order to drive the voice coils. Therefore, the transfer function of one actuator is derived to evaluate the FSM.

$$G(s) = \frac{\theta(s)}{F(s)} = \frac{d}{Is^2 + cs + k} \quad (4)$$

where I is the moment of inertia ($I = md^2$). The mirror mass is calculated according to its dimension and material properties (Pyrex).

$$V = \pi \cdot d^2 \cdot h \quad (5)$$

$$m = \rho V, \quad (6)$$

where V is the mirror volume, h is the thickness of the mirror, and ρ is the material density. It is necessary to take into account the friction between the mirror surface and the air. In such case, the friction coefficient c becomes:

$$c = uA, \quad (7)$$

where u is the air viscosity, A is the mirror surface area that is subject to a force exerted by the gas. The stiffness of the flexure hinge k is obtained from the mechanical model created with SolidWorks (shown in Fig. 4 and Fig. 5). According to all the parameters of the mirror assembly above, the transfer function (equations (3) and (4)) of the FSM model becomes as follows:

$$G(s) = \frac{\theta(s)}{F(s)} = \frac{4.959 \times 10^7}{s^2 + 130s + 102430} \quad (8)$$

As a first attempt to model the system, the frequency response of the FSM model is shown in Fig. 14. The Bode plot shows a resonant frequency at 48.8 Hz, which is lower than the other product (Newport, FSM-300) [25] because the real mirror parameters are not known and the model has been simplified from the available information.

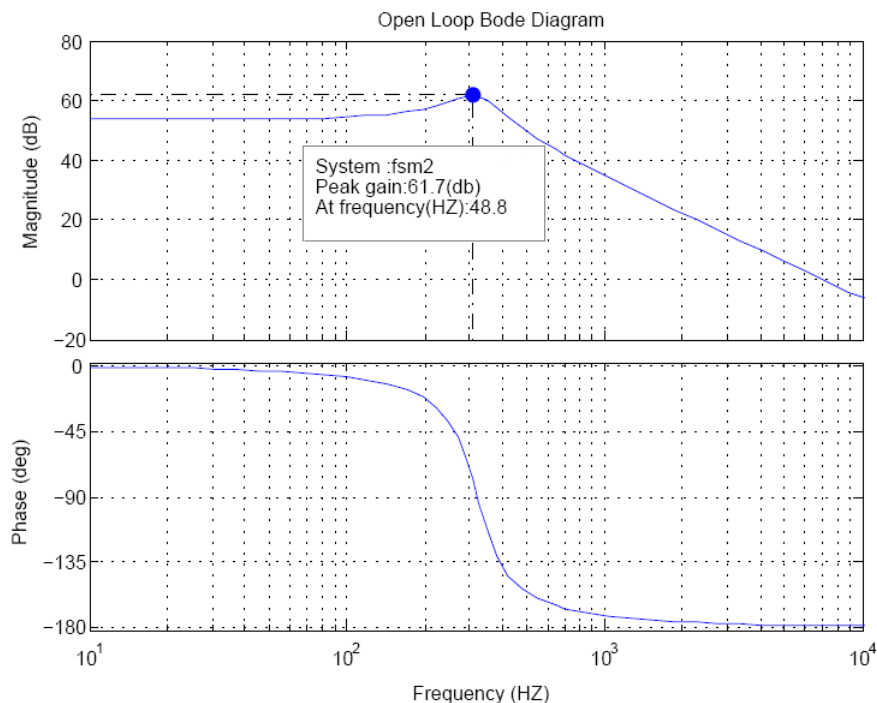


Fig. 14. FSM open loop analysis.

As shown in Fig. 9 and Fig. 11, although there are two axes, their control is independent of each other and is similar. Therefore, only one axis control design and simulation are discussed here. The PID controller is used since it is simple to implement and it has good performance with models representing 2nd order linear differential equations. The control loop is depicted in Fig. 15.

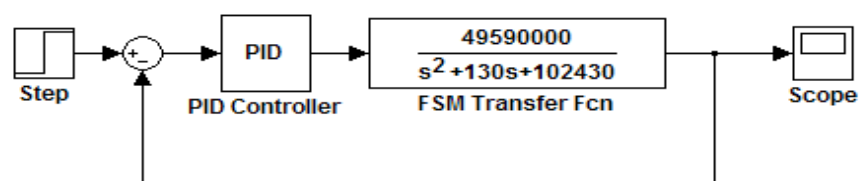


Fig 15. FSM closed loop analysis.

Based on the above control loop, using SISO control tools, the PID controller is calculated:

$$CC = \frac{0.0374(s^2 + 124s + 103000)}{s(s + 1760)} \quad (9)$$

The step response is shown in Fig. 16, which is the result of the PID controller tuning as given by Eq. 9. As shown in the figure, the system is stable. The frequency response of the FSM model with the derived controller is shown in Fig. 17 in order to simulate the controller CC. The Bode plots have the -3 dB point marked to show the bandwidth of the FSM system, which was found to be around 251 Hz.

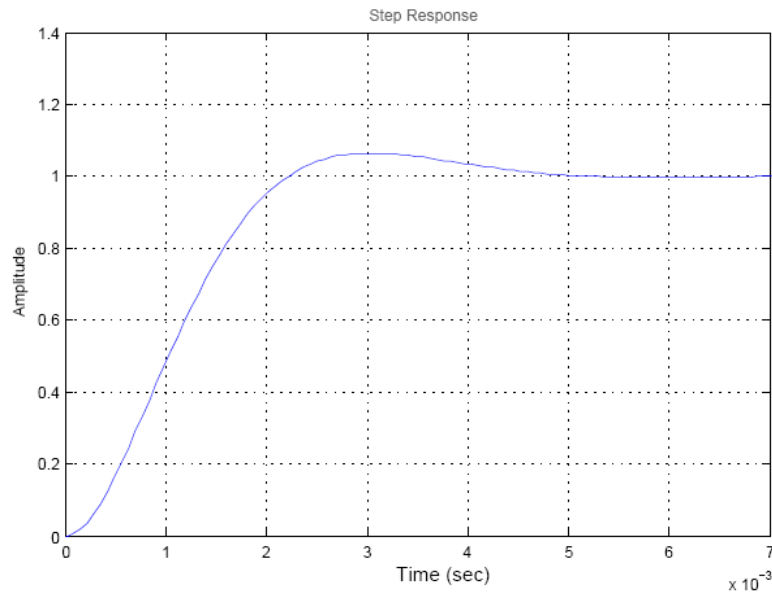


Fig. 16. Step response.

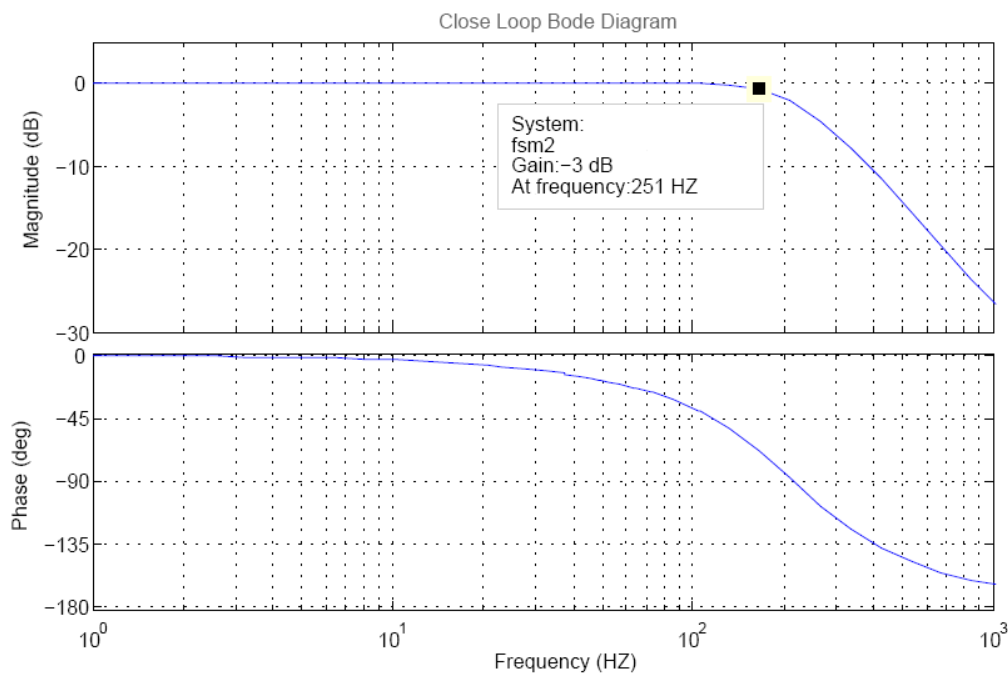


Fig. 17. Closed loop Bode diagram.

A comparison between Fig. 14 and Fig. 17 shows that the closed loop bandwidth exceeds that of the FSM. This is of course not true in reality, but the model and method are used in the simulations in order to adjust the controller as a comparison with the experimental results. The FSM model and the closed loop have been analyzed and they represent the real system under the assumptions made for the FSM parameters.

Once the theoretical model and ideal controller were designed, we determined the response of the actual FSM system using the dSPACE interface to provide the signal. The open loop response of the actual system is depicted in Fig. 18.

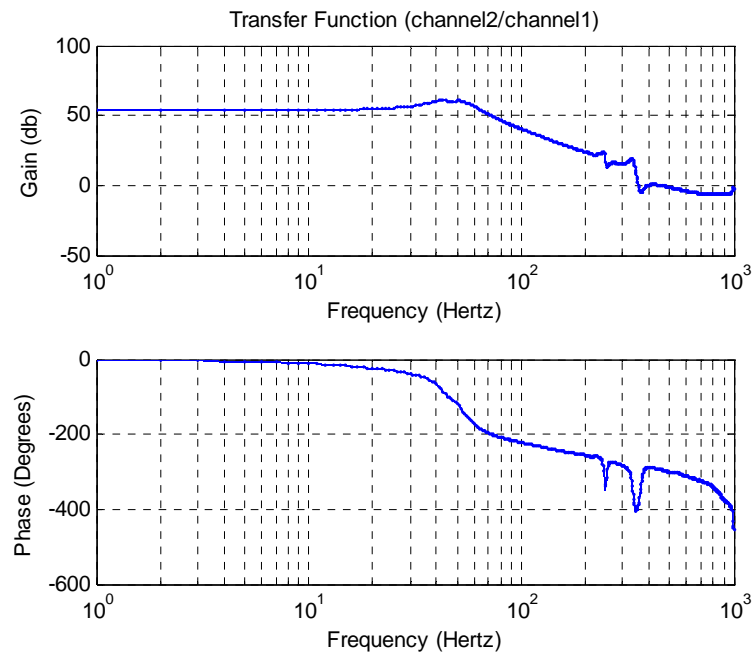


Fig. 18. Open loop experimental response of one axis.

With the aid of the open loop response experiments, we can obtain the FSM system open loop transfer function as follows:

$$G(s) = \frac{24722732570.3844}{(s + 498.5)(s^2 + 123.3s + 99370)} \quad (10)$$

Based on the above control method, using SISO control tools, the PID controller transfer function is also calculated:

$$CC = \frac{0.00021732(s + 508)(s^2 + 121s + 97600)}{s(s + 4365)} \quad (11)$$

The step response and the frequency response of the closed loop control with the actual FSM system are shown in Fig. 19. The bandwidth of the FSM system is around 260 Hz.

A comparison between Fig. 17 and Fig. 19 shows that the theoretical model of the system and the controller design method used in the simulations are very close to the experimental results. Therefore, the FSM model represents the real system under the assumptions made for the FSM parameters.

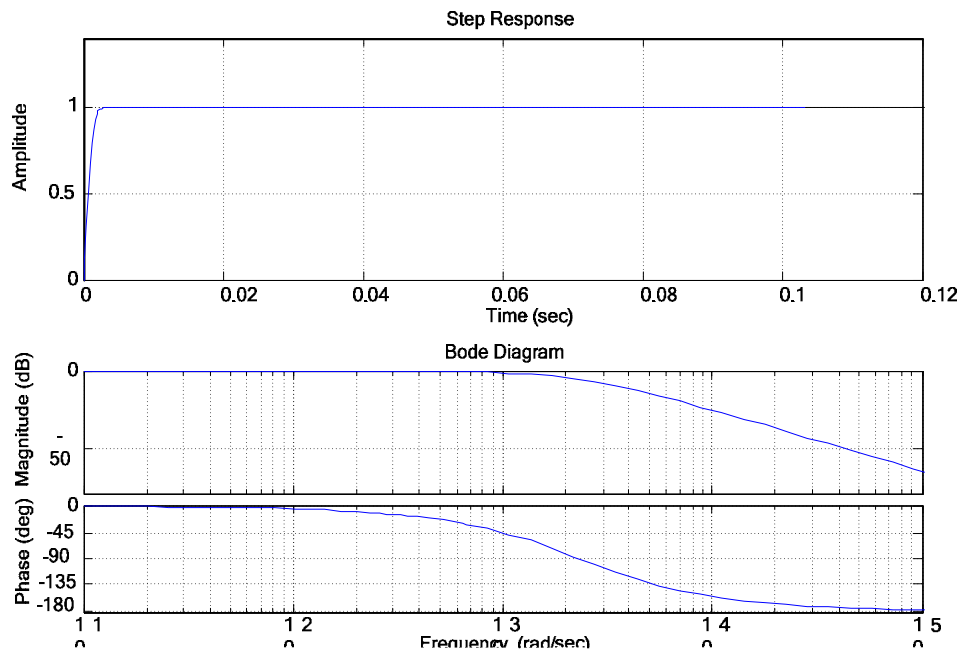


Fig. 19. Closed loop experimental response of one axis.

4. Conclusions

Precision laser beam steering is critical in numerous military and industrial applications. The jitter disturbance problem is the core problem of steering performances. This paper presented the possible precision laser beam steering technologies for optical steering. The research outlined the advantages of introducing compliant mechanism structures in the FSM and the design of a full steering system. The next steps will involve testing of the full setup and design controllers to compensate the pointing error. For the purpose of researching large-travel dimensional compliant mechanisms for precision positioning and key technologies, the performance of the FSM will be extensively tested in the laboratory in order to fully characterize the final tip-tilt loop. It is necessary to describe the functions and capabilities of the test facility that is used to test, model, and evaluate electro-optical components for applications ranging from laser communications to precision pointing and control systems.

The FSM model and closed loop are derived and the Bode diagrams are compared in order to make clear the design considerations and the difference between the model assumptions and the experimental results. The comparison between the measured gain response and the simulation model of the FSM should reveal similarity between the theoretical simulation model and the real system and offer a way to improve the model in order to better resemble the actual system.

The design method of building a beam steering system using a FSM based on compliant mechanisms and electromagnetic actuators to maintain precise laser beams steering control is feasible. Additional tests will be performed with the platform using MEMS mirrors as adaptive optics to research the wavefront problem integrated with the steering problem.

Acknowledgements

This work was carried out with the help of many colleagues in the Department of Mechatronic Engineering, National University of Defense Technology in China, and the Robotics and Mechatronics Laboratory, Department of Mechanical and Aerospace Engineering, The George Washington University. The authors would also like to thank the China Scholarship Council.

References

- [1]. R. W. Cochran, R. H. Vassar, Fast Steering Mirrors in Optical Control Systems, in *SPIE Proceedings: Advances in Optical Structure Systems*, Orlando, FL, 16-19 Apr. 1990, Vol. 1303, pp. 245-251.
- [2]. L. R. Hedding, R. A. Lewis, Fast steering mirror design and performance for stabilization and single axis scanning, *Proc. SPIE*, Vol. 1304, 1990, pp. 14-24.
- [3]. A. A. Portillo, G. G. Ortiz, C. Racho, Fine Pointing Control for Optical Communications, in *IEEE Proceedings of 'Aerospace Conference*, MT, USA, 10-17 March 2001, Vol. 3, pp. 3/1541 -3/1550.
- [4]. K. J. Held, J. D. Barry, Precision optical pointing and tracking from spacecraft with vibrational noise, *Proc. SPIE*, Vol. 616, 1986. pp. 160-173.
- [5]. Q. Wang, K. Chen, C. Y. Fu, Method for controlling fast-steering mirror driven by voice coil motor based on the closed-loop performance, *Opto-Electronic Engineering*, Vol. 32, Issue 2, 2005, pp. 9-11.
- [6]. V. A. Skormin, T. E. Busch, M. A. Givens, Model Reference Control of a Fast Steering Mirror of a Pointing, Acquisition and tracking System for Laser Communications, in *Proceedings of the IEEE 1995 National*, Vol. 2, 1995, pp. 907-913.
- [7]. A. Skormin, Mak A. Tascillo, T. E. Busch, Adaptive jitter rejection technique applicable to airborne laser communication systems, *Opto-Electronic Engineering*, Vol. 34, Issue 5, 1995, pp. 1263-1268.
- [8]. B. L. Wilkerson, Concepts for Fast Acquisition in Optical communication Systems, in *Proc. SPIE*, Vol. 6304, 2006, pp. 63040A. 1-63040A. 12.
- [9]. E. A. Watson, D. Miller, P. F. McManamon, Applications and requirements for non-mechanical beam steering in active electro-optic sensors, *Proc. SPIE*, Vol. 3633, 1999, pp. 216-225.
- [10]. T. Jono, M. Toyoda, K. NaKagawa, A. Yamamoto, Acquisition, tracking, and pointing systems of OJCETS for free-space laser communications, *Proc. SPIE*, Vol. 3692, 1999, pp. 41-50.
- [11]. R. Tyson, Introduction to adaptive optics, *SPIE Press*, USA, 2000.
- [12]. R. J. Watkins, B. N. Agrawal, Y. S. Shin, and H. J. Chen, Jitter control of space and airborne laser beams, in *Proceedings of the Conference on International Communications Satellite Systems Conference*, Monterey, CA: AIAA, May 2004, pp. 1.
- [13]. A Opto-Electronic, Do you know Acousto-Optics?, Application Notes. Available: (http://www.quanta-tech.com/Documentation/AO_Doc.pdf).
- [14]. OKO Technologies, Adaptive Optics Product Guide. Available: (<http://www.okotech.com/content/oko/pics/gallery/catWWW2.pdf>).
- [15]. L. M. Germann, A. Gupta, Inertial Line-of-Sight Stabilization Using Fine Steering Mirrors, in *Proceedings of the Conference on 'American Astronautical Society Guidance and Control Conference'*, Vol. 66, 1988.
- [16]. L. M. Germann, Advanced Two-Axis Beamsteering Element, in *Proceedings of the Conference on American Astronautical Society Guidance and Control Conference*, Vol. 63, 1985.
- [17]. L. L. Howell, Compliant mechanisms, *John Wiley & Sons Inc.*, 2001.
- [18]. N. Lobontiu, Compliant mechanisms: design of flexure hinges, *CRC Press*, 2003.
- [19]. CVI Melles Griot, Fundamentals of Beam Positioning, (http://www.mellesgriot.com/pdf/X_43_12-14.pdf).
- [20]. Electro-Optical Systems Inc., Quadrant receiver module. Available: (<http://www.eosystems.com/pdf/IGA-010-QUAD-E4.pdf>).
- [21]. Optics In Motion LLC. Available: (<http://www.opticsinmotion.net/index.html>)
- [22]. M. J. Xie, J. G. Ma, C. Y. Fu, Design and experiment of a LQ controller used in high-bandwidth fast-steering mirror system, *Proc. SPIE*, Vol. 4025, 2000, pp. 250.
- [23]. P. V. Mitchell, P. B. Griffith, D. K. Henderson, Fast-steering mirrors improve active beam stabilization. Available: (www.newsport.com/fsm).
- [24]. NASA Glenn Research Center, Air Properties Definitions. Available: (<http://www.lerc.nasa.gov/WWW/K-12/airplane/airprop.html>) .
- [25]. Newport, FSM-300 Datasheet. Available: (http://newport.com/file_store/PDFs/tempPDFs/e3881_Fast-Steering-Mirrors.pdf).